

DFTT 10/99
HUB-EP-99/13
March 1999

Non-perturbative states in the 3D ϕ^4 theory

M. Caselle^{a*}, M. Hasenbusch^{b†} and P. Provero^{c,‡}

^a *Dipartimento di Fisica Teorica dell'Università di Torino and
Istituto Nazionale di Fisica Nucleare, Sezione di Torino
via P.Giuria 1, I-10125 Torino, Italy*

^b *Humboldt Universität zu Berlin, Institut für Physik
Invalidenstr. 110, D-10115 Berlin, Germany*

^c *Dipartimento di Scienze e Tecnologie Avanzate
Università del Piemonte Orientale, Alessandria, Italy*

Abstract

We show that the spectrum of the three dimensional ϕ^4 theory in the broken symmetry phase contains non-perturbative states. We determine the spectrum using a new variational technique based on the introduction of operators corresponding to different length scales. The presence of non-perturbative states accounts for the discrepancy between Monte Carlo and perturbative results for the universal ratio ξ/ξ_{2nd} . We introduce and study some universal amplitude ratios related to the overlap of the spin operator with the states of the spectrum. The analysis is performed for the ϕ^4 theory regularized on a lattice and for the Ising model. This is a nice verification of the fact that universality reaches far beyond critical exponents. Finally, we show that the spectrum of the model, including non-perturbative states, accurately matches the glueball spectrum in the \mathbb{Z}_2 gauge model, which is related to the Ising model through a duality transformation.

*e-mail: caselle@to.infn.it

†e-mail: hasenbus@physik.hu-berlin.de

‡e-mail: provero@to.infn.it

1 Introduction

The idea of universality and the perturbative analysis of ϕ^4 theories have proved to be very powerful tools in the study of several statistical mechanics models (see *e.g.* Ref. [1] and references therein). In particular, with the advent of the last generation of high precision simulations for the three dimensional Ising model, an impressive agreement has been found between numerical results and perturbative predictions from ϕ^4 theory. Almost all universal quantities, both critical indices and amplitude ratios, agree within error bars [2]. With one small exception. The ratio between the "true" exponential correlation length ξ and the second moment one ξ_{2nd} which is predicted to be $\xi/\xi_{2nd} \sim 1.0065$, from a ϕ^4 calculation in the broken symmetric phase [3, 4], turns out to have a larger value $\xi/\xi_{nd} \sim 1.031(6)$ both from Montecarlo simulations and from low temperature expansions in the three dimensional Ising model. This paper deals with this discrepancy. We shall show that it can be understood as due to the presence of new non-perturbative states in the spectrum of the theory. We shall also evaluate various universal ratios involving masses and overlap constants of the non-perturbative states of the spectrum.

The analysis of the spectrum has been performed by a variational method, by introducing a set of operators analogous to the one introduced in Ref. [5] in the context of lattice gauge theories. These operators correspond to different length scales and are constructed recursively. We were able to identify precisely the first states of the spectrum. This new method (which is not restricted to the Ising case, but can be easily extended to any spin model) is among the main results of this paper and we shall discuss it in great detail.

We shall then show that universality holds also for this non trivial part of the spectrum, by directly simulating the lattice version of the ϕ^4 theory and again finding the same pattern of non-perturbative states and the same values of the universal ratios. Finally, we shall show, by using duality in the Ising model that these new states coincide with the lowest excitations of the glueball spectrum of the (dual) \mathbb{Z}_2 gauge model.

We will also present a detailed study of some universal amplitude ratios related to the overlap of the spin operator with the low-lying states of the transfer matrix. In particular, we will define and study a universal amplitude R which involves the overlap of the spin operator on the lowest state: for this quantity we can compare numerical results with perturbative calculations,

which we extend to two loop level.

This paper is organized as follows: in Sec. 2 we introduce the Ising and ϕ^4 models and the observables we will be interested in. In Sec. 3 and Sec. 4 we introduce two universal quantities ξ/ξ_{2nd} and R (related to the overlap constant of the spin operator) and discuss the existing numerical and analytical results about these two quantities, including their perturbative evaluation which we have extended to two loop level. In Sec. 5 we describe the new variational method we have used to determine the spectrum. Sec. 6 contains our Monte Carlo results for the spectrum of the model obtained with the variational approach: these results show unambiguously the existence of a non-perturbative state. In Sec. 7 we discuss duality and the relationship with the glueball spectrum of the \mathbb{Z}_2 gauge model. In Sec. 8 the spin-spin correlation function is reconsidered taking into account the existence of non-perturbative states in the spectrum; a new universal quantity R_2 is introduced, which is related to the overlap constant of the spin operator on the lowest non-perturbative state. Finally Sec. 9 is devoted to some concluding remarks, and in the Appendix we collect the details of the perturbative calculations.

2 The models and the observables

2.1 Ising model

The Ising model is defined by the action

$$S_{Ising} = -\beta \sum_{\langle n,m \rangle} s_n s_m , \quad (1)$$

where the field variable s_n takes the values -1 and $+1$; $n \equiv (n_0, n_1, n_2)$ labels the sites of a simple cubic lattice and the notation $\langle n, m \rangle$ indicates that the sum is taken on pairs of nearest neighbour sites only. The coupling β is proportional to the inverse temperature, $\beta \equiv \frac{1}{kT}$. We shall consider in the following n_1 and n_2 as “space” directions and n_0 as the “time” direction and shall sometimes denote the time coordinate n_0 with τ . The high and low T phases are separated by a critical point at a coupling whose value is known with very high precision [6]: $\beta_c = 0.2216543(2)(2)$. A peculiar property of the Ising model, which will play an important role in the following, is

the existence of an exact duality transformation which relates it to the \mathbb{Z}_2 gauge model. This transformation is known as Kramers–Wannier duality and relates the two partition functions:

$$\begin{aligned} Z_{gauge}(\beta) &\propto Z_{spin}(\tilde{\beta}) \\ \tilde{\beta} &= -\frac{1}{2} \log [\tanh(\beta)] \quad , \end{aligned} \tag{2}$$

where $\tilde{\beta}$ will be denoted in the following as the “dual coupling”. Using the duality transformation it is possible to build a one-to-one mapping of physical observables of the gauge system into the corresponding spin quantities. In particular the inverse of the mass of the lowest state in the spectrum of the gauge model ξ_{gauge} is mapped into the correlation length of the spin Ising model ξ .

2.2 ϕ^4 model

The lattice version of the ϕ^4 model is given by the action

$$S_{\Phi} = -\beta \sum_{\langle n,m \rangle} \phi_n \phi_m + \sum_n \phi_n^2 + \lambda \sum_n (\phi_n^2 - 1)^2 , \tag{3}$$

where now the field variable ϕ_n assumes all possible real values. In the limit $\lambda \rightarrow \infty$ the standard Ising model is recovered. In the space spanned by the two coupling constants (β, λ) the model has a second order critical line which belongs to the same universality class as the Ising model. In fact the two models share the same \mathbb{Z}_2 global symmetry which is broken in the low T phase. A peculiar feature of this model is that by suitably tuning λ one can reach a point in which the corrections to scaling (proportional to $\xi^{-\omega}$) disappear (see Refs. [6, 7]). It turns out that the optimal value is $\lambda = 1.1$. With this choice the critical coupling is [7] $\beta = 0.3750966(4)$.

We shall be interested in the exponential and second moment correlation lengths in the broken symmetry phase. Their definition is the same for the Ising and ϕ^4 models.

2.3 Exponential correlation length.

The exponential correlation length is defined in terms of the long distance behavior of the connected two point function:

$$\frac{1}{\xi} = - \lim_{|\vec{n}| \rightarrow \infty} \frac{1}{|\vec{n}|} \log \langle s_{\vec{0}} s_{\vec{n}} \rangle_c . \quad (4)$$

Note that for the ϕ^4 model s has to be replaced by ϕ . It is convenient to study the so called time slice correlation functions: The magnetization of a time slice is given by

$$S_{n_0} = \frac{1}{L^2} \sum_{n_1, n_2} s_{(n_0, n_1, n_2)} . \quad (5)$$

Let us define the time slice correlation function

$$G(\tau) = \sum_{n_0} \{ \langle S_{n_0} S_{n_0 + \tau} \rangle - \langle S_{n_0} \rangle^2 \} . \quad (6)$$

The large distance behavior of $G(\tau)$ is given by

$$G(\tau) = c \exp(-\tau/\xi) , \quad (7)$$

where ξ is the exponential correlation length, and c is a constant. The constant c is related to the overlap of the spin operator with the eigenstate of the transfer matrix corresponding to the lowest eigenvalue. A universal ratio involving the constant c will be discussed in Sec. 4.

It is important to stress that for small values of τ one expects deviations from this asymptotic behavior. These corrections are due to higher masses in the spectrum. A common tool to extract ξ is the so called effective correlation length

$$\xi_{eff}(\tau) = \frac{1}{\ln(G(\tau+1)) - \ln(G(\tau))} . \quad (8)$$

The effective correlation length is a monotonically increasing function of τ . In the limit $\tau \rightarrow \infty$ it converges to the exponential correlation length ξ . Notice that in a Monte Carlo simulation with increasing τ also the statistical errors of ξ_{eff} become larger. Therefore a fast convergence is important for the numerical study. It turns out that ξ_{eff} in the broken phase of the Ising

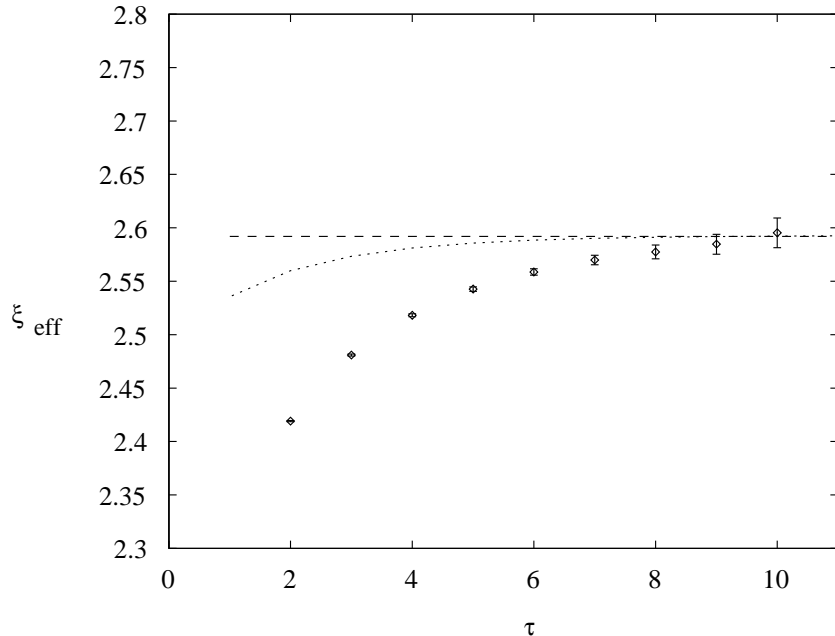


Fig. 1: Data for $\xi_{eff}(\tau)$ at $\beta = 0.2275$ (taken from Ref. [2]). The dashed line corresponds to the asymptotic value $\xi = 2.592$ (see Tab. 1). The dotted line corresponds to the function ξ_{pert} defined in Sec. 3.4

model is not a good estimator of ξ , since it requires distances larger than 3ξ to approach ξ with a relative accuracy of 1% (see Ref. [2] for a discussion of this point).

This is clearly visible in Figs. 1 and 2 where data taken from [2] are plotted. In particular in Fig. 1 we have shown the data for ξ_{eff} corresponding to $\beta = 0.2275$ while in Fig. 2 all the data of Ref. [2] are plotted together after a suitable rescaling. It is possible to see from Fig. 2 that all the data show the same (non-asymptotic) behavior in the range $\xi \leq \tau \leq 3\xi$. This shows that scaling is fulfilled in this range and that the deviation from the asymptotic behavior is certainly due to some physical reason (namely to the presence of nearby masses in the spectrum) and not to lattice artifacts.

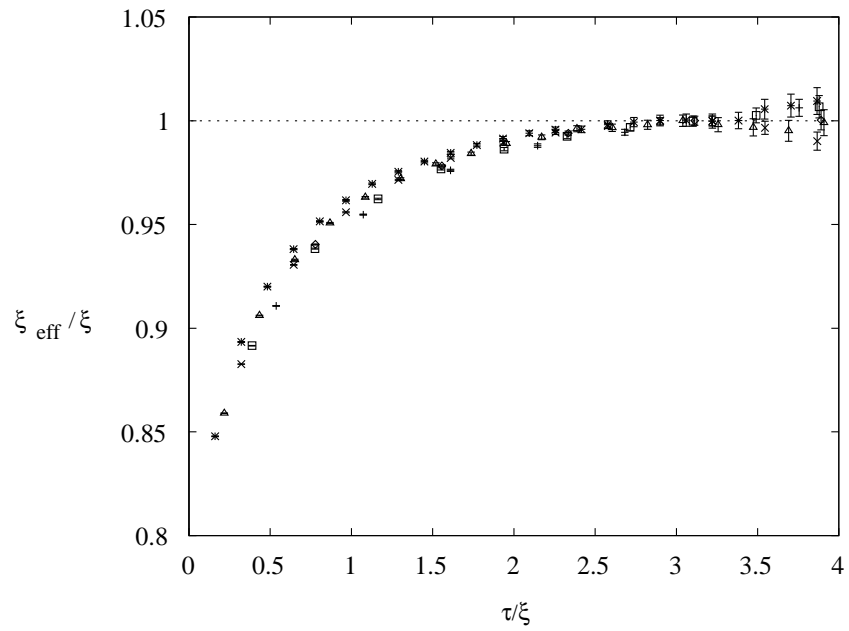


Fig. 2: $\xi_{eff}(\tau)$ for $\beta = 0.23910, 0.23142, 0.2275, 0.2260, 0.2240$. All the data are taken from Ref. [2]. Both ξ_{eff} and the distance τ are normalized, for each β , to the asymptotic value ξ .

2.4 Second moment correlation length.

The square of the second moment correlation length is defined for a d -dimensional model by

$$\xi_2^2 = \frac{\mu_2}{2d\mu_0} , \quad (9)$$

where

$$\mu_0 = \lim_{L \rightarrow \infty} \frac{1}{V} \sum_{m,n} \langle s_m s_n \rangle_c \quad (10)$$

and

$$\mu_2 = \lim_{L \rightarrow \infty} \frac{1}{V} \sum_{m,n} (m-n)^2 \langle s_m s_n \rangle_c , \quad (11)$$

where the connected part of the correlation function is defined by

$$\langle s_m s_n \rangle_c = \langle s_m s_n \rangle - \langle s_m \rangle^2 \quad (12)$$

and V is the lattice volume.

This estimator for the correlation length is very popular since its numerical evaluation (say in Monte Carlo simulations) is simpler than that of the exponential correlation length. Moreover it is the length scale which is directly observed in scattering experiments. However it is important to stress that it is not exactly equivalent to the exponential correlation length. We shall discuss the relation between the two in the next section.

3 The ξ/ξ_{2nd} ratio

3.1 ξ versus ξ_{2nd}

The relation between ξ and ξ_{2nd} can be obtained by noticing that we can rewrite μ_2 as follows

$$\begin{aligned} \mu_2 &= \frac{1}{V} \sum_{n,m} (n-m)^2 \langle s_m s_n \rangle_c \\ &= \frac{1}{V} \sum_{n,m} \sum_{\mu=0}^{d-1} (n_\mu - m_\mu)^2 \langle s_m s_n \rangle_c \\ &= \frac{d}{V} \sum_{n,m} (n_0 - m_0)^2 \langle s_m s_n \rangle_c \quad . \end{aligned} \quad (13)$$

Due to the exponential decay of the correlation function this sum is convergent and we can commute the spatial summation with the summation over configurations so as to obtain

$$\mu_2 = d \sum_{\tau=-\infty}^{\infty} \tau^2 \langle S_0 S_\tau \rangle_c \quad , \quad (14)$$

with S_{n_0} given by Eq. (5). Analogously one obtains

$$\mu_0 = \sum_{\tau=-\infty}^{\infty} \langle S_0 S_\tau \rangle_c \quad . \quad (15)$$

If we now insert these results in Eq. (9), we obtain

$$\xi_{2nd}^2 = \frac{\sum_{\tau=-\infty}^{\infty} \tau^2 G(\tau)}{2 \sum_{\tau=-\infty}^{\infty} G(\tau)} \quad . \quad (16)$$

Assuming a multiple exponential decay for $G(\tau)$,

$$\langle S_0 S_\tau \rangle_c \propto \sum_i c_i \exp(-|\tau|/\xi_i) \quad , \quad (17)$$

and replacing the summation by an integration over τ we get

$$\xi_{2nd}^2 = \frac{1}{2} \frac{\int_{\tau=0}^{\infty} d\tau \tau^2 \sum_i c_i \exp(-\tau/\xi_i)}{\int_{\tau=0}^{\infty} d\tau \sum_i c_i \exp(-\tau/\xi_i)} = \frac{\sum_i c_i \xi_i^3}{\sum_i c_i \xi_i} \quad , \quad (18)$$

which is equal to ξ^2 if only one state contributes.

An interesting consequence of this analysis is that the deviation of the ratio ξ/ξ_{2nd} from the value 1 gives an idea of the density of the lowest states of the spectrum. Note that $c_i \geq 0$ (see Eq. (40)) and therefore $\xi/\xi_{2nd} \geq 1$. If these are well separated the ratio will be very close to one, while a ratio significantly higher than one will indicate a denser distribution of states.

Notice that besides a discrete sum of exponentials (each corresponding to a pole in the Fourier transform of $G(\tau)$) we can also have an integral over a continuous set of exponential functions, which corresponds to a cut in the Fourier transform. This is the case, for instance, for the ϕ^4 model above the pair production threshold at $p = 2m$. These cuts can be thought of as

the coalescence of infinitely nearby exponentials, and actually, on a finite lattice, this is their correct description, since the transfer matrix has only a finite number of eigenvalues. The effect of these cuts is, as it happens for the isolated states, to enhance the ratio ξ/ξ_{2nd} . We shall refer to the contribution to the connected correlator due to these terms as the “cut contribution”.

3.2 MC estimates

Rather precise estimates for ξ_{2nd} can be found in Ref. [2] for various values of β in the scaling region of the $3D$ Ising model. In the same paper estimates for ξ also appear. However, while ξ_{2nd} can be extracted rather easily from MC simulations, the determination of ξ is much more delicate since, as we discussed above, it requires the identification of an asymptotic exponential decay. If other states besides the lowest one are present in the spectrum of the theory (and this is exactly the situation in which we are interested here) they can shadow the asymptotic behavior that we are looking for and produce systematic errors in the estimate of ξ (this problem was discussed in great detail in Ref. [2]).

A natural way out of this problem is to use a variational analysis to separate the various states in the spectrum (see [5]). However this requires a wide set of operators with a good overlap with the low-lying states of the theory. Constructing these operators is a highly non trivial task in the Ising model and has never been attempted up to now (we shall address and solve this problem in Sec. 5 below). Fortunately in the case of the $3D$ Ising model there is a nice way to avoid this obstacle. By using duality we can map the Ising model into an equivalent \mathbb{Z}_2 gauge model. In the gauge model one can easily construct, by looking at Wilson loops (namely products of gauge variables along closed contours) of various size and shape, a set of operators fulfilling the above requirements and perform a precise variational analysis of the spectrum. This route was followed in Ref. [8] leading to the results reported in Tab. 1. From them we extract the estimate $\xi/\xi_{2nd} = 1.031(6)$ obtained ignoring the first value, which is too far from the critical region, and taking a weighted sum of the remaining values (hence assuming that the correction to scaling terms are negligible within the errors for this ratio).

Table 1: Comparison of the results for the exponential correlation length obtained directly in the Ising model without a variational analysis (fourth column, data taken from Ref. [2], denoted as ξ_{eff}) and those obtained in the dual \mathbb{Z}_2 gauge model with a variational analysis (third column, data taken from Ref. [8], denoted as ξ_{gauge}). $\tilde{\beta}$ denotes the dual of β and is reported for completeness in the first column. In the fifth column we report the values for ξ_{2nd} obtained in Ref. [2] and finally in the last column the ratio ξ_{gauge}/ξ_{2nd} that we consider as our best estimate for ξ/ξ_{2nd} .

$\tilde{\beta}$	β	ξ_{gauge}	ξ_{eff}	ξ_{2nd}	ξ_{gauge}/ξ_{2nd}
0.72484	0.23910	1.296(3)	1.2851(28)	1.2335(15)	1.051(4)
0.74057	0.23142	1.864(5)	1.8637(45)	1.8045(21)	1.033(4)
0.74883	0.22750	2.592(5)	2.578(7)	2.5114(31)	1.032(3)
0.75202	0.22600	3.135(9)	3.103(7)	3.0340(32)	1.033(4)
0.75632	0.22400	4.64(3)	4.606(13)	4.509(6)	1.029(8)

3.3 Series expansion

It is possible to obtain an estimate for the ratio ξ/ξ_{2nd} by using the low temperature series published in Ref. [9]. This analysis has been recently performed in Ref. [10] with the result $\xi/\xi_{2nd} = 1.031(5)$.

3.4 Perturbative result

In the framework of the ϕ^4 theory we naively expect only one mass in the spectrum (hence only one isolated exponential in $G(\tau)$). However it is easy to see that this result is true only at tree level and that at one loop, a cut appears in the Fourier transform of the propagator, starting from twice the value of the fundamental mass. As mentioned above this exactly coincides with the pair production threshold. The corresponding expression for $G(\tau)$ (which we shall call in the following $G(\tau)_{pert}$) is [4]:

$$G(\tau)_{pert} = \frac{1}{2m_{ph}L^2} e^{-m_{ph}\tau} \left[1 + \frac{1}{32} \frac{u_R}{4\pi} \right]$$

$$+ \frac{3u_R}{16\pi L^2 m_{ph}} \int_{2m_{ph}}^{\infty} d\mu \frac{e^{-\mu\tau}}{\mu \left(1 - \frac{\mu^2}{m_{ph}^2}\right)^2} . \quad (19)$$

where u_R denotes the dimensionless renormalized coupling, m_{ph} is the physical mass, defined as the location of the zero of the inverse correlator in momentum space $G^{-1}(p)$ and coinciding with the inverse of the exponential correlation length ξ (for all the details and definitions concerning perturbative results, see the Appendix).

Eq. (19) shows that even perturbatively the long distance behavior of time slice correlations is not purely exponential: this, as discussed in the previous section, implies a ratio ξ/ξ_{2nd} different from 1. Indeed, defining the renormalized mass m_R as the inverse propagator in momentum space at $p = 0$, so that $m_R = 1/\xi_{2nd}$, one finds at one loop [3, 4]

$$\frac{\xi}{\xi_{2nd}} = \frac{m_R}{m_{ph}} = 1 - \frac{u_R}{4\pi} \left(\frac{13}{32} - \frac{3}{8} \log 3 \right) . \quad (20)$$

The fixed point value u_R^* of the renormalized coupling has been recently estimated in a high precision Monte Carlo simulation [2] to be $u_R^* = 14.3(1)$. Plugging this result into Eq. (20) we obtain the universal value

$$\frac{\xi}{\xi_{2nd}} = 1.00652(3) , \quad (21)$$

a result which is rather far from the Monte Carlo one.

A similar exercise is to define the function ξ_{pert} by inserting $G_{pert}(\tau)$ in Eq. (8) and compare it to the Monte Carlo results for ξ_{eff} . This comparison is shown in Fig. 1. Again, it appears that the perturbative contribution alone is not enough to justify the deviation of ξ_{eff} from its asymptotic value.

We have extended the calculation of ξ/ξ_{2nd} to two loop level; details are given in the Appendix. The result is

$$\frac{\xi}{\xi_{2nd}} = 1 + 0.00573 \frac{u_R}{4\pi} + 0.00474 \frac{u_R^2}{16\pi^2} . \quad (22)$$

If we plug in the fixed point value $u_R^* = 14.3$ we obtain

$$\frac{\xi}{\xi_{2nd}} \sim 1.01266 . \quad (23)$$

One can see that the convergence properties of the series are not very satisfactory. Since at the fixed point $u_R/4\pi = 1.14$, the two loop contribution is as big as 94% of the one loop term. Therefore this result must be taken with great caution. Taking it at face value, we see that the two loop contribution goes in the right direction, but is not sufficient to close the gap between perturbative and Monte Carlo results.

These results seem to indicate that perturbative effects alone cannot explain the rather large value of ξ/ξ_{2nd} found in numerical simulations or, equivalently, the preasymptotic behavior of $\xi_{eff}(\tau)$. An unambiguous indication that such non-perturbative physics is actually present will be given by the determination of the spectrum of the transfer matrix by a variational method in Sec. 6.

4 Universal ratios of overlap amplitudes.

From the large distance behavior of the correlation function $G(\tau)$ we can extract, besides the ξ/ξ_{2nd} ratio, another universal quantity defined as follows. If we parameterize the large distance behavior of $G(\tau)$ as

$$G(\tau) = c \exp(-\tau/\xi) \quad , \quad (24)$$

then the ratio

$$R = \left(\frac{L}{\xi}\right)^2 \frac{c}{M^2} \quad (25)$$

(where L is the size of the lattice in the spacelike directions and M denotes the magnetization) is universal.

Since this amplitude combination is not among those usually discussed in the literature it is worthwhile to describe its meaning in more detail in the framework of quantum field theory and its relationship with the so called "overlap constants" .

Let us look, as an example, at ϕ^4 theory in three dimensions at tree level in the broken symmetry phase. The *point – point* connected correlator (normalized to the square of the mean magnetization) in momentum space is given by

$$\frac{\langle \phi(x)\phi(y) \rangle_c}{\langle \phi(0) \rangle^2} = \frac{|F_\phi|^2}{m} \int \frac{d^3p}{(2\pi)^3} \frac{e^{ip(x-y)}}{p^2 + m^2} \quad (26)$$

where F_ϕ denotes the projection of the ϕ field on the momentum basis and hence is usually referred to as the *overlap* of the ϕ field with the particle state of mass m .

Let us now turn to the slice-slice correlator. The slice operator is defined as

$$S(t) = \frac{1}{L^2} \int dx_1 dx_2 \phi(x_1, x_2, t) \quad . \quad (27)$$

Plugging this definition into Eq. (26) and performing the various integrals we find for connected slice-slice correlator $G(\tau)$:

$$G(\tau) \equiv \langle S(0)S(\tau) \rangle_c = \langle S(0) \rangle^2 \frac{|F_\phi|^2}{(mL)^2} e^{-m|\tau|} \quad . \quad (28)$$

Hence if we assume the large distance behavior of Eq. (24) we immediately recognize that the amplitude ratio defined in Eq. (25) exactly coincides with $|F_\phi|^2$.

This analysis can be straightforwardly extended to the case in which more than one massive state is present in the spectrum of the theory. If we expect (as in Eq. (17)) a multiple exponential decay for $G(\tau)$,

$$\langle S_0 S_\tau \rangle_c \propto \sum_i c_i \exp(-|\tau|/\xi_i) \quad , \quad (29)$$

then we can define an independent universal ratio for each state of the spectrum

$$R_i = \left(\frac{L}{\xi_i} \right)^2 \frac{c_i}{M^2} \quad (30)$$

which coincides with the (square of the) overlap amplitude F_ϕ^i , that is with the projections of the ϕ operator on the i^{th} massive state of the spectrum.

The F_ϕ^i 's encode much interesting information on the theory. In some cases, for instance for two dimensional integrable models, they can be evaluated exactly from the S-matrix of the models.

In the case of the three dimensional Ising model, no exact result is known, but it is possible to extract a perturbative estimate of R using the same results discussed in Sec. 3.4. We shall deal with this calculation in the next section.

4.1 Perturbative result

Looking at Eq. (19) we see that the constant c in front of the exponential is given at one loop by

$$c = \frac{1}{2m_{ph}L^2} \left[1 + \frac{u_R}{128\pi} \right] . \quad (31)$$

Plugging this result into Eq. (25), using the definition of the renormalized coupling (see Appendix)

$$u_R = \frac{3m_R}{M^2} , \quad (32)$$

we obtain

$$R = \frac{u_R}{6} \left[1 - \frac{u_R}{128\pi} \right] \quad (33)$$

so that at the fixed point $u_R^* = 14.3$

$$R \sim 2.298 . \quad (34)$$

Also this calculation can be extended to two loop level as shown in the Appendix; as in the case of the amplitude ratios ξ/ξ_{2nd} we find that the perturbative series has poor convergence properties. The result is

$$R = \frac{u_R}{6} \left(1 - 0.03125 \frac{u_R}{4\pi} - 0.02567 \frac{u_R^2}{16\pi^2} \right) \quad (35)$$

so that plugging in the fixed point value $u_R^* = 14.3$ we obtain

$$R \sim 2.219 . \quad (36)$$

4.2 MC estimate

It is easy to construct an estimator for the ratio R if we assume the value of the correlation length as an input. From Eqs. (24,25) we see that the quantity

$$R_{eff} = \left(\frac{L}{\xi} \right)^2 \frac{G(\tau) \exp(\tau/\xi)}{M^2} \quad (37)$$

converges to R for $\tau \rightarrow \infty$. The behavior of R_{eff} as a function of τ is similar to that of ξ_{eff} . At short distances it is a decreasing function of τ and then

reaches a stable plateau for $\tau \geq 3\xi$. This is clearly visible in Fig. 3 where data obtained for four values of β (the data are taken from Ref. [2]) are plotted together. It is interesting to notice that in the region $\xi \leq \tau \leq 3\xi$ all of the four samples follow the same curve, showing that the preasymptotic behavior of R is, like the one of ξ_{eff} , a physical effect rather than a lattice artifact. As in the case of ξ_{eff} , this behavior signals that the correlation function is not a single decaying exponential, hence the presence of higher states in the spectrum and interaction effects (cuts in the Fourier transform). We shall come back to this point in Sec. 7 below. We report in Tab. 2 the values of $R(\tau = 3\xi)$ which we consider as our best estimates for the asymptotic value of R . Let us briefly comment on how we obtained the numbers plotted in

Table 2: *The ratio R for various values of β .*

β	R
0.23142	2.072(24)
0.22750	2.068(18)
0.22600	2.060(30)
0.22400	2.082(50)

Fig. 3 and reported in Tab. 2. We used as input data the estimates of ξ reported in the third column of Tab. 1 (extracted from Ref. [8]) and used for $G(\tau)$ the high precision values obtained in [2]. The main source of error in R_{eff} comes from ξ . Due to the exponential in Eq. (37) it increases as a linear function of τ . This explains the rather large errors quoted in Tab. 2. As can be seen in Tab. 2 the estimates of R are stable within the errors as a function of β . A naive extrapolation (neglecting corrections to scaling) suggests the value $R = 2.07(4)$ at the fixed point, which shows a 10% and 7% deviation from the one and two loop perturbative estimates respectively.

As discussed in Sec. 3, the two loop perturbative evaluation of R is not very reliable due to its poor convergence. If one chooses to take it seriously, one is left with another discrepancy between two loop perturbative predictions and numerical results, that is another hint to the existence of non-perturbative states in the spectrum.

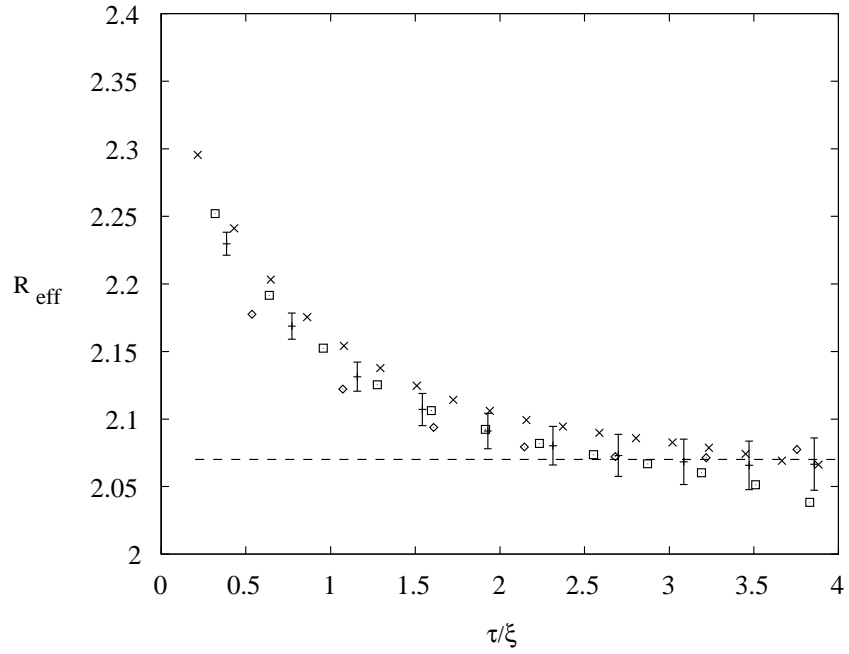


Fig. 3: $R_{\text{eff}}(\tau)$ for $\beta = 0.23142$ (diamonds), 0.2275 (pluses), 0.2260 (squares) and 0.2240 (crosses). All the data are taken from Ref. [2]. The distance t is normalized, for each β , to the asymptotic value ξ . To avoid confusion only the error bars for the $\beta = 0.2275$ data are reported, the other error bars are of the same size. The dashed line corresponds to the asymptotic value $R = 2.07$ quoted in Sec. 4.2

5 The variational method for the determination of the spectrum

As mentioned above, the only way to obtain reliable values for the masses of a complex spectrum like the one in the broken phase of the Ising model is to use a variational technique. Since this is one of the main points of our analysis we shall devote this section to a detailed discussion, first of the general features of the approach and second of the choice of the operators.

5.1 Variational analysis

In general the mass spectrum of a theory is given by the eigenvalues of the Hamiltonian H . On the lattice, one diagonalizes the transfer matrix T , which is the discrete version of e^{-H} . For a finite lattice the transfer matrix of the Ising model is a real symmetric matrix. Therefore it can be diagonalized. Let us denote the resulting eigenvalues by λ_i . Then the mass-spectrum is given by

$$m_i = -\log \left(\frac{\lambda_i}{\lambda_0} \right) , \quad (38)$$

where λ_0 is the largest eigenvalue of T . The basic strategy to evaluate these eigenvalues is to compute expectation values of certain correlation functions. Masses can then be determined from the decay of these correlation functions with the separation in time.

$$\begin{aligned} G_{AB}(\tau) &= \langle A(0)B(\tau) \rangle = \frac{\langle 0|AT^\tau B|0 \rangle}{\langle 0|T^\tau|0 \rangle} \\ &\sim \frac{1}{\lambda_0^\tau} \sum_i \langle 0|A|i \rangle \langle i|T^\tau|j \rangle \langle j|B|0 \rangle = \sum_i c_i^{AB} \left(\frac{\lambda_i}{\lambda_0} \right)^\tau \\ &= \sum_i c_i^{AB} \exp(-m_i\tau) , \end{aligned} \quad (39)$$

where $|i\rangle$ denotes the eigenstates of the transfer matrix and¹

$$c_i^{AB} = \langle 0|A|i \rangle \langle i|B|0 \rangle . \quad (40)$$

¹If $A = B = S(\tau)$ (where $S(\tau)$ is the slice operators defined above) then the constants c_i^{AB} coincide with the overall constants c_i defined in sect.4 .

The main problem in the numerical determination of masses is to find operators A and B that have a good overlap with a single state $|i\rangle$; *i.e.* such that c_i is large compared with c_j , $j \neq i$. A first simplification is obtained by using the so called “zero momentum” operators, namely operators obtained by summing over a slice orthogonal to the time direction, so that all c_i ’s that correspond to nonvanishing momentum vanish. The zero momentum operators are just the time slice averages introduced in Sec. 2.

A systematic way to further improve the overlap is to simultaneously study the correlators among several operators A_α . One must then measure all of the correlations among these operators and construct the cross-correlation matrix defined as:

$$C_{\alpha\beta}(\tau) = \langle A_\alpha(\tau)A_\beta(0) \rangle - \langle A_\alpha(\tau) \rangle \langle A_\beta(0) \rangle \quad . \quad (41)$$

By diagonalizing the cross-correlation matrix one can then obtain the mass spectrum.

This method can be further improved [5] by studying the generalized eigenvalue problem

$$C(\tau)\psi = \lambda(\tau, \tau_0)C(\tau_0)\psi \quad , \quad (42)$$

where τ_0 is small and fixed (say, $\tau_0 = 0$). Then it can be shown that the various masses m_i are related to the generalized eigenvalues as follows [5]:

$$m_i = \log \left(\frac{\lambda_i(\tau, \tau_0)}{\lambda_i(\tau + 1, \tau_0)} \right) \quad , \quad (43)$$

where both τ and τ_0 should be chosen as large as possible, $\tau \gg \tau_0$ and as τ is varied the value of m_i must be stable within the errors. Practically we are forced to keep $\tau_0 = 0$ to avoid too large statistical fluctuations and at the same time τ is generally forced to stay in the range $\tau = 1$ to 5. This method is clearly discussed in Refs. [5], to which we refer for further details. All the results that we shall list in the next section have been obtained with this improved method. In order to give some information on the reliability of the estimates we shall also list, besides the numerical values of the masses, the value of τ at which they have been evaluated.

5.2 The Operator Basis

While the formalism of the variational approach to compute the spectrum is quite general, a suitable set of operators to compute the correlation functions

has to be found for each model separately. Suitable in this context means that the wavefunctions of the small mass states are given to a good approximation by some linear combination of the operators selected.

In the case of the \mathbb{Z}_2 gauge model a good set operators for the 0^+ channel is formed by Wilson loops of various sizes [8]. We kept in the present analysis the basic idea that different operators should correspond to different length scales, and we included the standard time-slice magnetization in our basis of operators.

We came up with a recursive definition of the operators. The starting point is the field $\phi_{n_0, n_1, n_2}^{(0)} = \phi_{n_0, n_1, n_2}$ as it is generated by the Monte Carlo. In the case of the Ising model we similarly start with the definition $\phi_{n_0, n_1, n_2}^{(0)} = s_{n_0, n_1, n_2}$. Then the field (for each time-slice separately) is transformed according to the following rule:

$$\phi_{n_0, n_1, n_2}^{(n+1)} = \text{sign}(u) \left((1-w)|u| + wy \right) \quad (44)$$

with

$$u = r \phi_{n_0, n_1, n_2}^{(n)} + (1-r) \frac{1}{4} (\phi_{n_0, n_1-1, n_2}^{(n)} + \phi_{n_0, n_1+1, n_2}^{(n)} + \phi_{n_0, n_1, n_2-1}^{(n)} + \phi_{n_0, n_1, n_2+1}^{(n)}) \quad (45)$$

w , y and r being free parameters of the transformation. The operators are then given by the sum of the ϕ^n over a given time-slice (zero momentum projection)

$$S^{(n)}(n_0) = \sum_{n_1, n_2} \phi_{n_0, n_1, n_2}^{(n)} \quad (46)$$

The correlation matrix is then built by

$$C_{ij}(\tau) = \langle S(n_0)^{(i)} S(n_0 + \tau)^{(j)} \rangle - \langle |S(n_0)^{(i)}| \rangle \langle |S(n_0 + \tau)^{(j)}| \rangle \quad (47)$$

We performed test simulations with different choices for the parameters w , y and r for small correlation length both in the Ising and ϕ^4 models. The quality of the resulting operator basis was judged by looking at the convergence of effective masses towards their asymptotic values. It turned out that $r = 0$ is a good choice for ϕ^4 (for Ising we have to choose r slightly different from 0 to have a well defined transformation). Also there is no sharp constraint on the value of y . Mostly we have taken y equal to the magnetization. In the case of w it turned out that values close to 0 are a good choice. Note however that taking w exactly equal to 0 would result in all $S^{(n)}$ being equal.

6 The spectrum: Monte Carlo results

We simulated the Ising model in its low temperature phase at $\beta = 0.23142$ and 0.2275 , and the ϕ^4 model at fixed $\lambda = 1.1$ for the three values $\beta = 0.405$, 0.385 and 0.3798 . The two critical values of β are $\beta_c = 0.2216543(2)(2)$ and $\beta_c = 0.3750966(4)$ for the Ising model and the ϕ^4 theory at $\lambda = 1.1$ respectively. In both cases we used a single cluster algorithm [11]. For the application of cluster algorithms in ϕ^4 type models see Ref. [12].

We used cubic lattices with periodic boundary conditions and size L in both spatial directions (those which define the plane in which we perform the zero momentum projection of our observables) and chose a size $2L$ in the “time” direction in which we evaluate correlators. L was always chosen such that $L \geq 16\xi$. Some information on the simulations is collected in Tab. 2.

For the whole set of (zero momentum projected) improved operators $S^{(n)}(n_0)$ we computed the correlators $C_{i,j}(\tau)$ for all possible translations in the time direction. For the values of β closer to the critical point, we used the set of operators obtained by iterating twice the smoothing procedure described in the previous section. In all five simulations we found the same

Table 3: *Some information on the run in the low temperature phase of the Ising model. N_{op} denotes the number of operators used in the variational analysis, $N_{smoothing}$ the number of smoothing iterations between two operators.*

β	L	measures	sweeps/measure	$N_{smoothing}$	N_{op}
0.23142	$30^2 \times 60$	300000	20	1	20
0.2275	$45^2 \times 90$	500000	30	2	20

pattern:

- a] The data for the lowest mass are of much better quality than those extracted from the simple spin-spin correlator. This means in particular that we have a very precocious approach to the asymptotic result and always find a stable plateau starting from values of τ of the order of (or even smaller than) the correlation length. The quality of the data can

Table 4: *Some information on the run in the low temperature phase of the ϕ^4 model at $\lambda = 1.1$. N_{op} and $N_{smoothing}$ are defined as above.*

β	L	measures	sweeps/measure	$N_{smoothing}$	N_{op}
0.405	$20^2 \times 40$	2300000	10	1	12
0.385	$40^2 \times 80$	850000	15	2	20
0.3798	$60^2 \times 120$	250000	20	2	20

be better appreciated by looking at Fig. 4 where our data and those extracted from the pure spin-spin correlator are compared.

- b] In all cases we can detect the first excitation above the lowest mass and evaluate its mass with good precision. For the simulations farther from the critical point we can even detect the next excitation (see however the next section for a comment on the interpretation of this further state)
- c] In applying the variational approach discussed above we always chose $\tau_0 = 0$ while the distance τ at which the mass is measured varies from sample to sample and is reported for completeness in Tabs. 5 and 6.
- d] If we decrease the number of operators involved in the variational analysis our data smoothly reach those extracted from the pure spin-spin correlator. The rate of this approach gives an idea of the number of operators (and smoothing iterations) needed to obtain a good overlap with the states of the spectrum.
- e] On finite lattices there is no spontaneous symmetry breaking, because of finite action tunneling solutions. The effect of these solutions on the mass spectrum is to split each level into a nearly degenerate doublet (see *e.g.* Ref. [13] for a discussion of this point). This splitting is of order $\sqrt{\sigma}e^{-\sigma L^2}$, where σ is the interface tension and L the transverse size of the lattice. With our choices of parameters we have $\sigma L^2 \sim 30$ (cfr. Ref. [14] where the relevant values of σ are reported), therefore the splitting cannot be observed with our resolution.

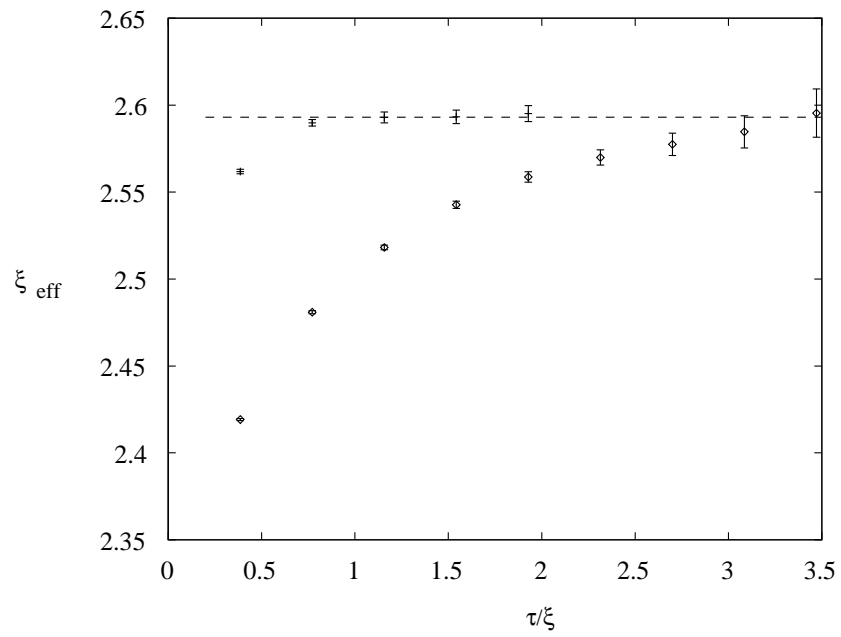


Fig. 4: Values of ξ_{eff} obtained with the variational method (pluses) and with the standard spin-spin correlator (diamonds) for $\beta = 0.2275$. The dashed line denotes the asymptotic value $\xi = 2.592$ (see Tab. 1). The distance τ is measured in units of ξ .

The values for the (inverse of the) masses that we found are reported in Tabs. 5 and 6. In order to address the issues of scaling and universality we

Table 5: *Correlation lengths extracted with the variational approach in the 3d Ising model. Below each mass we report the value of τ at which it has been evaluated. $\tau_0 = 0$ is always assumed. The question marks denote the fact that the corresponding states are not yet stable within the errors hence the values quoted must be better considered as lower bounds.*

β	ξ_1	ξ_2	ξ_3
0.23142	1.870(3) ($\tau = 3$)	1.027(7) ($\tau = 3$)	0.727(13) (?) ($\tau = 3$)
0.2275	2.593(4) ($\tau = 4$)	1.429(8) ($\tau = 4$)	1.016(13) (?) ($\tau = 4$)

Table 6: *Correlation lengths extracted with the variational approach in the 3d ϕ^4 model.*

β	ξ_1	ξ_2	ξ_3
0.405	1.1130(9) ($\tau = 2$)	0.609(2) ($\tau = 2$)	0.464(5) ($\tau = 2$)
0.385	2.182(2) ($\tau = 3$)	1.182(5) ($\tau = 3$)	0.872(9) ($\tau = 3$)
0.3798	3.463(4) ($\tau = 4$)	1.827(8) (?) ($\tau = 5$)	1.246(19) (?) ($\tau = 4$)

constructed the ratio of these masses with the lowest one.

These adimensional ratios should approach a constant as $\beta \rightarrow \beta_c$ and be universal, namely they should have the same value in the Ising and ϕ^4 models. This is clearly confirmed in Tab. 7 where we have reported these ratios for the two models together. A naive fit of these data (neglecting possible corrections

Table 7: Mass ratios for Ising and ϕ^4 models.

Model	β	ξ_1	ξ_1/ξ_2	ξ_1/ξ_3
ϕ^4	0.405	1.1130(9)	1.828(7)	2.40(3)
Ising	0.23142	1.870(3)	1.821(15)	2.57(5) (?)
ϕ^4	0.385	2.182(2)	1.846(10)	2.50(1)
Ising	0.2275	2.593(4)	1.815(13)	2.55(4) (?)
ϕ^4	0.3798	3.463(4)	1.895(10) (?)	2.78(5) (?)

to scaling and neglecting the values denoted with a question mark which must be considered only as upper bounds) gives the two results

$$\frac{m_2}{m_1} = 1.83(3) \quad , \quad \frac{m_3}{m_1} = 2.45(10) \quad . \quad (48)$$

It is important at this point to discuss the relationship of these results with the perturbative expansion in the ϕ^4 theory discussed in Sec. 3.4. The first excitation that we find above the lowest one is *below* the pair production threshold: therefore it cannot be a perturbative effect related to cuts in the Fourier transform. Hence it is a new non-perturbative state which exists in the spectrum of the two models and cannot be seen within the framework of a perturbative analysis.

On the contrary the second mass state could well be related to the cut. As a matter of fact, if we ignore the power tail in the functional expression of the cut and try to mimic it with a simple exponential we would exactly find a fictitious state with a mass of approximately 2.4 times the lowest one [4]. This state could well be identified with the third mass that we measure in our analysis.

7 Duality and the Glueball spectrum

As already noticed in Sec. 2.1 the correlation length of the Ising model is related by duality to the (inverse of the) mass of the 0^+ glueball of the \mathbb{Z}_2 gauge model. It is natural to conjecture that the new states that we have found in the spectrum of the Ising model are related by duality to the remaining

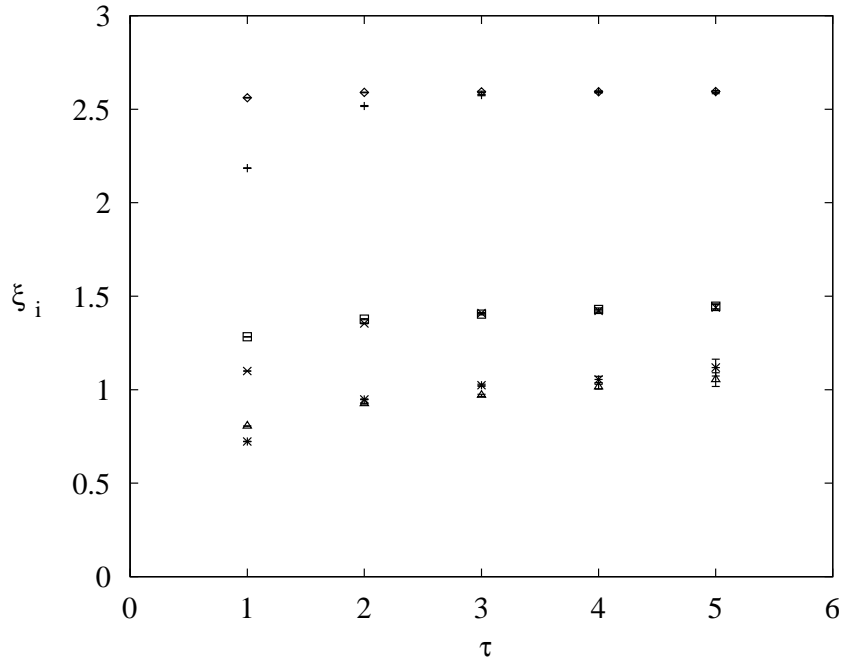


Fig. 5: Comparison between the spectrum obtained with the variational method in the Ising model at $\beta = 0.2275$ and the values of the masses in the 0^+ family of the 3D \mathbb{Z}_2 gauge model at the dual coupling $\beta = 0.74883$. Diamonds, squares and triangles denote ξ_1, ξ_2 and ξ_3 respectively, while pluses, crosses and stars denotes the $0^+, 0^{+'}$ and $0^{+''}$ glueballs.

states of the 0^+ family. This conjecture is strongly supported by our data. In particular it is impressive to compare the values of ξ_{eff} obtained in this paper as a function of the separation τ with the corresponding observables for the glueball states $0^+, 0^{+'}, 0^{+''}$ obtained in Ref. [8]. This comparison is shown in Fig. 5 for the value $\beta = 0.2275$. While for the first two values of τ (which are dominated by the lattice artifacts) we find large discrepancies, for $\tau \geq 3$ the two sets of data remarkably agree within the errors. This identification is further supported by the values of the mass ratios extrapolated to the continuum limit, which again agree within the errors (see Tab. 8).

Table 8: Mass ratios for the Ising model and \mathbb{Z}_2 gauge model. The results for the gauge model are taken from Ref. [8]

Mass ratio	Ising model	\mathbb{Z}_2 gauge model
ξ_1/ξ_2	1.83(3)	1.88(2)
ξ_1/ξ_3	2.45(10)	2.59(4)

8 The spin-spin correlator revisited.

Once the spectrum has been understood we can again address the behavior of the spin-spin correlator. In order to clarify our analysis we devote the following two sections 8.1 and 8.2 to a detailed discussion of $G(\tau)$ in the particular case of the Ising model at $\beta = 0.2275$ where both data from Ref. [2, 8] and from the present variational analysis exist. To allow the reader to reproduce our analysis we report in Tab. 9 the values of the connected spin-spin correlator which were obtained in Ref. [2] (to which we refer for information on the parameters of the simulations and the algorithm used).

8.1 Overlap amplitudes

In Sec 4.2 we constructed an estimator R_{eff} for the universal ratio R . The slow convergence of R_{eff} to its asymptotic value, shown in Fig. 3, was explained as originating from higher mass states in the spectrum and cut effects. Now that the low-lying part of the spectrum has been determined by the variational method, the preasymptotic behavior of the correlation function $G(\tau)$ is under control. This information allows us to construct a new estimator of R with better convergence properties. Moreover, the presence of non-perturbative states in the spectrum makes it natural to define and study new universal quantities related to the overlap of the spin operator on these states, that are the exact analogs of R for the new states.

As discussed in the previous section, our results for the spectrum show a non-perturbative state with a mass of about 1.8 times the fundamental one, and a third state that could be another non-perturbative state or a perturbative interaction effect (cut), or a superposition of the two. These

Table 9: The connected correlator $G(\tau)$ at $\beta = 0.2275$. The data are taken from Ref. [2]. In the first column we report the distance τ in units of the lattice spacing and in the second column the value of $G(\tau) \times 10^5$.

τ	$G(\tau) \times 10^5$
0	152.30447(5)
1	98.57691(4)
2	65.20074(4)
3	43.57136(4)
4	29.29125(3)
5	19.76683(3)
6	13.37177(3)
7	9.06161(3)
8	6.14757(3)
9	4.17518(3)
10	2.84039(3)
11	1.93695(3)
12	1.32855(3)

two possibilities correspond to two different ansatze for the functional form of $G(\tau)$: The first one (that we shall call in the following the “three mass ansatz”) is:

$$G(\tau) = c_1 \exp(-\tau/\xi_1) + c_2 \exp(-\tau/\xi_2) + c_3 \exp(-\tau/\xi_3) \quad . \quad (49)$$

This choice does not make use of any perturbative information on the theory, and is based on the only assumption that higher states, which are certainly present, are beyond our resolution, *i.e.* their contribution is of the same order of magnitude as our statistical errors and hence cannot be taken into account.

The second possibility (that we shall call in the following the “two mass plus cut ansatz”) is based on the assumption that the third state we see in the spectrum is not a new state but the effect of the cut, that is a perturbative effect due to the self interaction of the fundamental state.

$$G(\tau) = c_1(\exp(-\tau/\xi_1) + f_{cut}(\tau/\xi_1)) + c_2 \exp(-\tau/\xi_2) \quad . \quad (50)$$

and f_{cut} given by Ref. [4]

$$f_{cut}(\tau) = \frac{3}{2} \frac{u_R}{4\pi} \int_{\frac{2}{\xi}}^{\infty} d\mu \frac{e^{-\mu\tau}}{\mu(1-\mu^2\xi^2)^2} . \quad (51)$$

Here we are approximating the cut contribution with its one loop expression. Again, we assume that higher states in the spectrum are beyond our resolution.

We shall show below that the results obtained with these two choices essentially coincide. Thus, with the data at our disposal, we cannot select between the two scenarios, but at the same time we are sure that this systematic uncertainty does not affect our results for ξ_1 , c_1 , ξ_2 and c_2 .

With the constants c_i obtained in this way we may construct estimators for the universal quantities: we define

$$R_i^{eff}(\tau) = \left(\frac{L}{\xi_i}\right)^2 \frac{c_i^{eff}(\tau)}{M^2} \quad (52)$$

with $i = 1, 2, 3$ or $i = 1, 2$ according to the ansatz. The functions $c_i^{eff}(\tau)$ are determined from the Monte Carlo value of $G(\tau)$ for three or two nearby values of τ and from the values of the masses as determined from the variational method. R_1^{eff} is our new, improved estimator of the universal ratio R , while R_2^{eff} and R_3^{eff} are estimators for the new universal ratios associated with the new states. Let us discuss in detail the results obtained with the two ansatze.

8.1.1 The three mass ansatz

The results may be summarized as follows:

- The asymptotic estimate of R is consistent with the one obtained in Sec. 4.2 with the unimproved estimator R_{eff} , but R_1^{eff} reaches its asymptotic value already for $\tau \sim \xi$ (see Fig. 6).
- Despite the fact that the presence of the higher masses and the related new degrees of freedom slightly increases the systematic uncertainty in the function $R_1^{eff}(\tau)$ the error on the estimate of R is slightly smaller than that quoted in Tab. 2. This is due to the fact that we can extract

our asymptotic estimate already at $\tau \sim \xi$, where the statistical uncertainties on $G(\tau)$ are smaller. Since the major source of uncertainty comes from the error in the estimate of ξ_1 and gives a contribution which increases linearly with τ this improvement compensates the above uncertainty. Our final result is $R = 2.055(15)$ (to be compared with the value $R = 2.068(18)$ obtained with the unimproved estimator).

- The function $R_2^{eff}(\tau)$ shows a stable behavior in the range $\xi \leq \tau \leq 2\xi$ (see Fig. 7) and a reliable estimate of R_2 can be extracted. The result is affected by errors (which are mainly due to the uncertainty in ξ_1) larger than those which affect R . Our final result is $R_2 = 0.45(8)$.
- The function $c_3(\tau)$ never stabilizes and it is impossible to extract a reliable asymptotic estimate for R_3 .

8.1.2 The two mass plus cut ansatz.

Again using as input parameters the values of ξ_1 and ξ_2 extracted from the variational analysis we may construct from pairs of nearby values of $G(\tau)$ the functions $R_1^{eff}(\tau)$ and $R_2^{eff}(\tau)$. We find the following results:

- The behavior of $c_1^{eff}(\tau)$ is essentially unaffected by the change of ansatz (see Fig. 6). Our best estimate for R_1 does not change.
- The function $R_2^{eff}(\tau)$ is more affected by the change, but in the region $\xi \leq \tau \leq 2\xi$ where the data reach a stable plateau the new estimate agrees within the errors with those obtained with three masses (see Fig. 7). Our estimate in this case is $R_2 = 0.55(5)$.

Thus we may conclude that the interpretation of the third mass as a cut is compatible with the data and suggests a slightly higher value for R_2 .

Trying to take into account the systematic error involved in the choice of the two ansatz we give as our final result:

$$R = 2.055(15) \qquad R_2 = 0.50(10) \qquad (53)$$

which is a suitable combination of the two estimates.

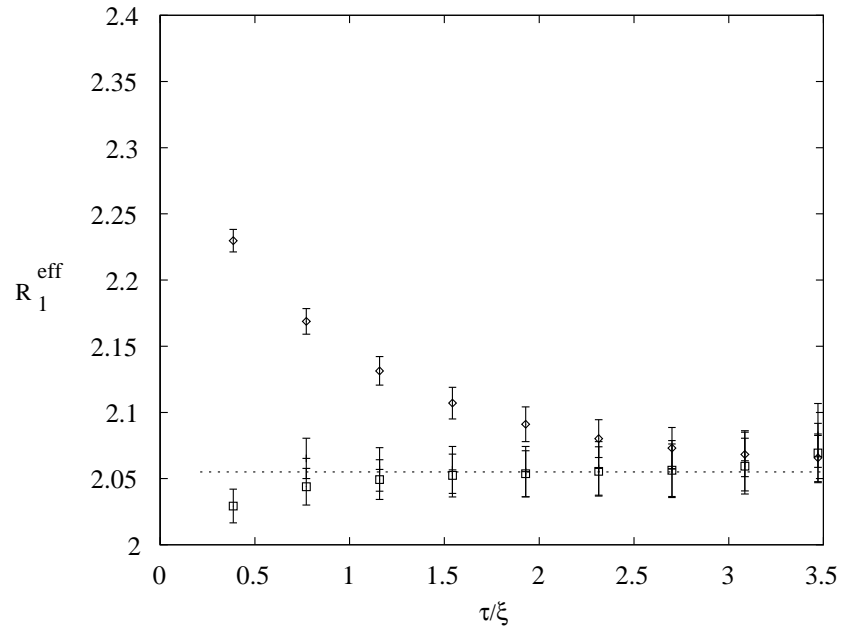


Fig. 6: The improved estimator $R_1^{\text{eff}}(\tau)$ derived from the three mass ansatz (pluses) and the two mass plus cut ansatz (squares). Also shown for comparison is the unimproved estimator $R_{\text{eff}}(\tau)$ defined in Sec. 4 (diamonds). The data are at $\beta = 0.2275$ and the distance τ is measured in units of ξ .

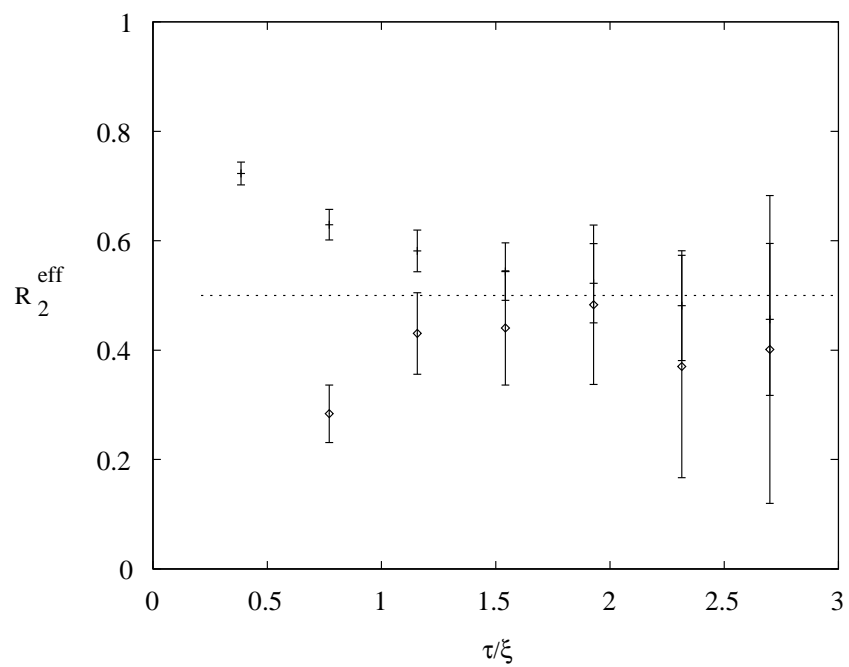


Fig. 7: Values of R_2 obtained assuming the three mass ansatz (diamonds) and the two mass plus cut ansatz (pluses) for $\beta = 0.2275$. The distance τ is measured in units of ξ .

8.2 The behavior of $\xi_{eff}(\tau)$.

As a final test of our results, let us now turn our attention to the function $\xi_{eff}(\tau)$ and test if, from the knowledge of the spectrum and the overlap constants, we are able to reproduce the observed behavior of $\xi_{eff}(\tau)$. Since the two ansatze discussed above give essentially equivalent results we have chosen to do this test with the two mass plus cut ansatz only. We have constructed our best estimate of the correlator, inserting into the equation:

$$G^{th}(\tau) = c_1(\exp(-\tau/\xi_1) + f_{cut}(\tau/\xi_1)) + c_2 \exp(-\tau/\xi_2) \quad . \quad (54)$$

our best estimates for c_1, c_2, ξ_1 and ξ_2 reported in Eq. (53) and Tab. 5 respectively. Then we constructed:

$$\xi^{th}(\tau) = \frac{1}{\ln(G^{th}(\tau + 1)) - \ln(G^{th}(\tau))}; \quad (55)$$

The result is compared with the observed $\xi_{eff}(\tau)$ in Fig. 8. All the data for $\tau \geq \xi$ agree within the error bars. For comparison, we show also the purely perturbative prediction.

8.3 Continuum limit.

In Sec. 4.2 we have shown that the ratio R has a good scaling behavior and we extracted an estimate of its value in the continuum limit. It is very important to test if also the ratio R_2 has good scaling properties. To this end we have studied its value for two other values of β : $\beta = 0.2260$, $\beta = 0.2240$, using again the data of Ref. [2]. Let us briefly motivate this choice and the procedure we used:

- We chose these two samples because for values of β higher than $\beta = 0.2275$ the value of ξ_2 becomes so small that it is impossible to observe its overlap with the techniques discussed above.
- In the analysis we need the values of ξ_1, ξ_2 and ξ_3 . which we have not evaluated explicitly in this paper in the two cases $\beta = 0.2260$, $\beta = 0.2240$. However, as shown in Sec. 7, duality allows us to identify ξ_1, ξ_2 and ξ_3 with the masses of the first three states in the 0^+ family of the glueball spectrum of the \mathbb{Z}_2 gauge model, which we evaluated, precisely for these values of β , in Ref. [8].

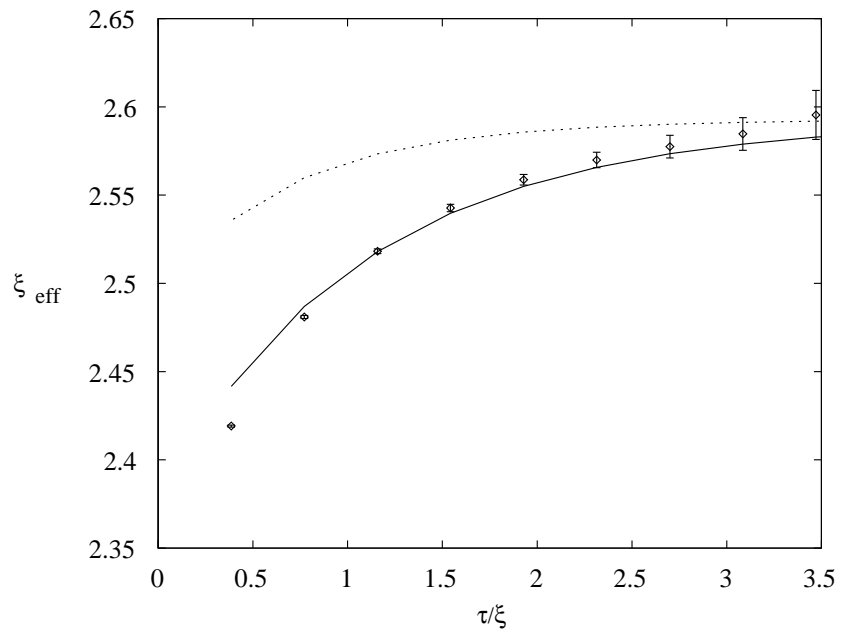


Fig. 8: Data for $\xi_{eff}(\tau)$ at $\beta = 0.2275$ (taken from Ref. [2]). The solid line corresponds to the function ξ_{th} defined in Sec. 8.2 The dotted line corresponds to the function ξ_{pert} defined in Sec. 3.4. The distance τ is measured in units of ξ .

We performed the same analysis discussed in the previous section and found analogous results, that is:

- The estimates of the ratio R obtained with the unimproved and improved estimators are consistent; the improved estimator allows one to reach the asymptotic value at much shorter distances.
- For each β , the values for R_2 obtained assuming the two extreme situations: the three mass and the two mass plus cut ansatz agree within the errors in the range $\xi \leq \tau \leq 2\xi$.
- In this same range, the estimate of R_2 show a perfect scaling behavior as a function of β . All the values obtained for the three different samples and the two possible ansatz agree within the errors and fall into the window $R_2 = 0.5 \pm 0.1$ (see Fig. 9).

8.4 Universality.

Another important issue is to see if we find in the ϕ^4 model the same values for R and R_2 that we obtained in the Ising case. To answer this question we analyzed the data for the two samples nearest the critical point, along the line discussed above. For $\tau \sim \xi$, choosing the three mass ansatz we obtained the results reported in Tab. 10. For the value of β nearest the critical point we find a perfect agreement with the Ising results.

Table 10: R_1 and R_2 in the ϕ^4 model, using to the three mass ansatz.

β	R_1	R_2
0.385	1.981(30)	0.75(40)
0.3798	2.047(20)	0.59(20)

9 Conclusions

In this paper we have developed a new variational method to study the spectrum of statistical models. We applied it to the three dimensional Ising and

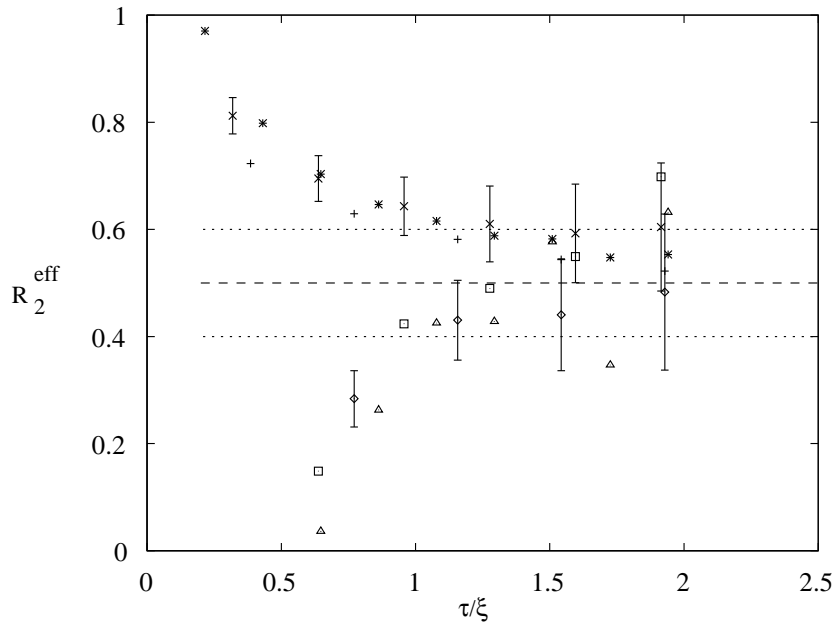


Fig. 9: Values of R_2 obtained assuming the three mass ansatz for $\beta = 0.2275$ (diamonds), $\beta = 0.2260$ (squares) and $\beta = 0.2240$ (triangles), compared with those obtained with the two mass plus cut ansatz (pluses for $\beta = 0.2275$, crosses for $\beta = 0.2260$ and stars for $\beta = 0.2240$). The distance t is measured in units of ξ . All the data are taken from Ref. [2]. The distance τ is normalized, for each β , to the asymptotic value ξ . To avoid confusion only the error bars for the $\beta = 0.2275$ data are reported, the other error bars are of the same size. The dashed line corresponds to the asymptotic value $R_2 = 0.5(1)$ quoted in Sec. 8.1.

ϕ^4 models and succeeded in detecting two states beyond the lowest mass excitation. For these new states we could give a rather precise estimate of the mass and, for the lowest of them, also of the overlap constant. By comparing our results with those published in Refs. [2, 8] we reach the following conclusions:

- The state denoted in the paper as ξ_2 , which is the first one above the lowest mass, has a truly non-perturbative nature.
- The next state, denoted in the paper as ξ_3 , could again be a non-perturbative excitation, but the data are also compatible with a perturbative origin: it could be the signature of the infinite set of states above the threshold for pair production of the lowest mass state.
- The non-perturbative states offer a natural explanation for the disagreement between perturbative predictions and Montecarlo results for the universal quantities ξ/ξ_{2nd} and R .
- We have been able to extract estimates for the adimensional ratios: ξ_2/ξ_1 , ξ_3/ξ_1 , R , R_2 which show a good scaling behavior as functions of β .
- *Universality* holds for the entire spectrum of the model. The states that we observe in the 3d Ising model appear with the same masses and overlap constants also in the ϕ^4 model.
- *Duality* holds for the entire spectrum of the model. The states that we observe in the Ising spin model are related by duality to the glueballs of the 0^+ family of the $3D \mathbb{Z}_2$ gauge model.

Appendix: Perturbative calculations at two loop order

We consider the 3D Euclidean field theory defined by the action

$$S = \int d^3x \left[\frac{1}{2} \partial_\mu \phi \partial_\mu \phi + \frac{g}{24} (\phi^2 - v^2)^2 \right] \quad (56)$$

which we want to treat perturbatively around the stable solution

$$\phi = v . \quad (57)$$

Therefore we define the fluctuation field φ :

$$\phi = v + \varphi \quad (58)$$

in terms of which the action is

$$S = S_0 + S_I , \quad (59)$$

where

$$S_0 = \int d^3x \left[\frac{1}{2} \partial_\mu \varphi \partial_\mu \varphi + \frac{m^2}{2} \varphi^2 \right] \quad (60)$$

$$S_I = \int d^3x \left[\frac{m\sqrt{g}}{2\sqrt{3}} \varphi^3 + \frac{g}{24} \varphi^4 \right] \quad (61)$$

$$m^2 = \frac{gv^2}{3} . \quad (62)$$

From this expression we can read the Feynman rules in momentum space:

$$\text{---} = \frac{1}{p^2+m^2} ; \quad \text{---} \langle \text{---} = -m\sqrt{3g} ; \quad \text{---} \times \text{---} = -g$$

We will need the one and two point correlation functions of the φ field at two loop order; the diagrammatic expansions are:

$$\begin{aligned} \langle \varphi \rangle &= \text{---} \bullet \text{---} = \frac{1}{2} \text{---} \bigcirc \text{---} + \frac{1}{4} \text{---} \bigcirc \bigcirc \text{---} + \frac{1}{4} \text{---} \bigcirc \text{---} \bigcirc \text{---} \\ &+ \frac{1}{6} \text{---} \bigcirc \text{---} \bigcirc \text{---} + \frac{1}{4} \text{---} \bigcirc \text{---} \bigcirc \text{---} + \frac{1}{8} \text{---} \bigcirc \text{---} \bigcirc \text{---} + \frac{1}{4} \text{---} \bigcirc \text{---} \bigcirc \text{---} \end{aligned}$$

and

$$\begin{aligned}
\langle \varphi \varphi \rangle_c &= \text{[Diagram: Solid black circle]} = \text{[Diagram: Horizontal line]} + \frac{1}{2} \text{[Diagram: Circle on top of line]} + \frac{1}{2} \text{[Diagram: Circle on bottom of line]} \\
&+ \frac{1}{2} \text{[Diagram: Circle on top of line]} + \frac{1}{4} \text{[Diagram: Two circles on top of line]} + \frac{1}{6} \text{[Diagram: Circle with horizontal line through center]} + \frac{1}{4} \text{[Diagram: Two circles on top of line]} + \frac{1}{4} \text{[Diagram: Two circles on top of line]} \\
&+ \frac{1}{8} \text{[Diagram: Circle on top of line]} + \frac{1}{4} \text{[Diagram: Circle with horizontal line through center]} + \frac{1}{4} \text{[Diagram: Two circles on top of line]} + \frac{1}{4} \text{[Diagram: Two circles on top of line]} + \frac{1}{6} \text{[Diagram: Circle with horizontal line through center]} \\
&+ \frac{1}{4} \text{[Diagram: Two circles on top of line]} + \frac{1}{2} \text{[Diagram: Circle on top of line]} + \frac{1}{4} \text{[Diagram: Two circles on top of line]} + \frac{1}{4} \text{[Diagram: Two circles on top of line]} + \frac{1}{4} \text{[Diagram: Circle on top of line]} \\
&+ \frac{1}{2} \text{[Diagram: Circle with horizontal line through center]} + \frac{1}{4} \text{[Diagram: Two circles on top of line]} + \frac{1}{4} \text{[Diagram: Two circles on top of line]} + \frac{1}{4} \text{[Diagram: Circle on top of line]} + \frac{1}{2} \text{[Diagram: Circle with horizontal line through center]} \\
&+ \frac{1}{4} \text{[Diagram: Two circles on top of line]} + \frac{1}{4} \text{[Diagram: Two circles on top of line]} + \frac{1}{4} \text{[Diagram: Two circles on top of line]} + \frac{1}{2} \text{[Diagram: Circle with horizontal line through center]} + \frac{1}{2} \text{[Diagram: Circle on top of line]} \\
&+ \frac{1}{4} \text{[Diagram: Two circles on top of line]} + \frac{1}{2} \text{[Diagram: Circle on top of line]} + \frac{1}{4} \text{[Diagram: Two circles on top of line]} + \frac{1}{8} \text{[Diagram: Two circles on top of line]} + \frac{1}{4} \text{[Diagram: Circle with horizontal line through center]}
\end{aligned}$$

All of the relevant integrals have been calculated in dimensional regularization by Rajantie in Ref. [15], where one can also find the explicit expression of the one particle irreducible part of the two point function. We obtain for $d = 3 - 2\epsilon$

$$\langle \phi \rangle = v + \langle \varphi \rangle = v \left[1 + \frac{1}{2} \frac{u}{4\pi} + \frac{u^2}{16\pi^2} \left(\frac{1}{12} + \frac{1}{24\epsilon} + \frac{1}{12} \log \frac{\mu^2}{9m^2} \right) \right] , \quad (63)$$

where μ is an arbitrary mass scale and u is the dimensionless bare coupling $u \equiv g/m$; the two point connected function gives

$$\langle \phi(x)\phi(y) \rangle - \langle \phi \rangle^2 = \langle \varphi(x)\varphi(y) \rangle_c = \int \frac{d^3p}{(2\pi)^3} G(p) e^{ip(x-y)} \quad (64)$$

with

$$G^{-1}(p) = p^2 + m^2 + \frac{u}{4\pi} m^2 \left(1 - \frac{3m}{2p} \arctan \frac{p}{2m} \right)$$

$$\begin{aligned}
& + \frac{u^2}{16\pi^2} m^2 \left[\frac{1}{12\epsilon} + \frac{1}{6} \log \frac{\mu^2}{9m^2} - \frac{4p^2 + 25m^2}{4(p^2 + 4m^2)} \frac{m}{p} \arctan \frac{p}{3m} \right. \\
& + \frac{2p^4 + 35m^2p^2 + 54m^4}{24p^2(p^2 + 4m^2)} \log \left(1 + \frac{p^2}{9m^2} \right) + \frac{p^2 + 10m^2}{4(p^2 + 4m^2)} \\
& + \frac{3}{4} \frac{m^2}{p^2} \arctan^2 \frac{p}{2m} + \frac{3}{8} \log 3 \frac{m}{p} \arctan \frac{p}{2m} + \frac{3}{16} A \left(\frac{p}{m} \right) \\
& \left. - \frac{9}{2} B \left(\frac{p}{m} \right) \right] , \tag{65}
\end{aligned}$$

where $p \equiv \sqrt{p^2}$ and

$$\begin{aligned}
A(x) & \equiv \frac{i}{x} \left[\text{Li}_2 \left(-\frac{ix}{3} \right) + \text{Li}_2(-2 + ix) - \text{Li}_2 \left(\frac{ix}{3} \right) - \text{Li}_2(-2 - ix) \right] \tag{66} \\
B(x) & \equiv \frac{1}{x^2 \sqrt{x^2 + 3}} \int_0^1 dt \frac{1}{\sqrt{x^2 + 4 - t^2}} \left[\frac{2x}{2+t} \left(\arctan \frac{x}{2+t} - \arctan \frac{x}{2} \right) \right. \\
& \left. + \log \frac{x^2 + (2+t)^2}{(2+t)^2} \right] . \tag{67}
\end{aligned}$$

These correlation functions are used to fix three renormalization constants in order to compare the perturbative results with lattice data. We use the scheme introduced in Ref. [16], and define

$$G^{-1}(p) \equiv Z_R^{-1} (m_R^2 + p^2 + O(p^4)) \tag{68}$$

$$v_R \equiv Z_R^{-1/2} \langle \phi \rangle , \tag{69}$$

so that v_R is to be identified with the magnetization and m_R with $1/\xi_{2nd}$. Moreover it is useful to define

$$u_R \equiv 3 \frac{m_R}{v_R^2} , \tag{70}$$

corresponding to the scaling quantity:

$$\frac{3\chi}{\xi_{2nd}^3 M^2} , \tag{71}$$

where χ is the susceptibility and M is the magnetization.

From Eqs. (63,67) we find [17]

$$m_R^2 = m^2 \left[1 + \frac{3}{16} \frac{u}{4\pi} + \frac{u^2}{16\pi^2} \left(\frac{1}{12\epsilon} + \frac{1}{6} \log \frac{\mu^2}{9m^2} + \frac{7429}{20736} \right) \right] \quad (72)$$

and

$$u_R = u \left[1 - \frac{31}{32} \frac{u}{4\pi} + \frac{u^2}{16\pi^2} \left(-\frac{1}{24\epsilon} - \frac{1}{12} \log \frac{\mu^2}{9m^2} + \frac{40957}{55296} \right) \right] . \quad (73)$$

The physical mass m_{ph} is defined as the location of the pole of $G(p)$ on the imaginary axis, that is by imposing

$$G^{-1}(i m_{ph}) = 0 . \quad (74)$$

We find

$$\begin{aligned} m_{ph}^2 &= m^2 \left\{ 1 + \frac{u}{4\pi} \left(1 - \frac{3}{4} \log 3 \right) + \frac{u^2}{16\pi^2} \left[\frac{1}{12\epsilon} + \frac{1}{6} \log \frac{\mu^2}{9m^2} \right. \right. \\ &\quad + \frac{1}{4} - \frac{\pi^2}{64} - \frac{7}{4} \log 2 + \frac{4}{3} \log 3 + \frac{3}{16} \left(\log \frac{4}{3} \right)^2 \\ &\quad \left. \left. + \frac{3}{8} \text{Li}_2 \left(\frac{1}{4} \right) + \frac{3}{16} \text{Li}_2 \left(\frac{1}{3} \right) - \frac{9}{2} B(i) \right] \right\} \end{aligned} \quad (75)$$

so that, putting together Eqs. (72,73,75) we find

$$\begin{aligned} \frac{m_R}{m_{ph}} &= \frac{\xi}{\xi_{2nd}} = 1 + \frac{u_R}{4\pi} \left(-\frac{13}{32} + \frac{3}{8} \log 3 \right) \\ &\quad + \frac{u_R^2}{16\pi^2} \left[-\frac{2603}{165888} + \frac{\pi^2}{128} + \frac{7}{8} \log 2 - \frac{319}{384} \log 3 + \frac{27}{128} (\log 3)^2 \right. \\ &\quad \left. - \frac{3}{32} \left(\log \frac{4}{3} \right)^2 - \frac{3}{16} \text{Li}_2 \left(\frac{1}{4} \right) - \frac{3}{32} \text{Li}_2 \left(\frac{1}{3} \right) + \frac{9}{4} B(i) \right] , \end{aligned} \quad (76)$$

that is Eq. (22).

Finally, we are interested in the perturbative evaluation of the amplitude ratio R defined in Sec. 4, which is given by

$$R = \frac{iZ_R^{-1}}{m_{ph}^2 v_R^2} \lim_{p \rightarrow i m_{ph}} (p - i m_{ph}) G(p) . \quad (77)$$

The result is

$$R = \frac{u_R}{6} \left\{ 1 - \frac{1}{32} \frac{u_R}{4\pi} + \frac{u_R^2}{16\pi^2} \left[\frac{13295}{55296} + \frac{11}{4} \log 2 + \frac{9}{8} B(i) - \frac{103}{48} \log 3 + \frac{15}{128} (\log 3)^2 \right] \right\} , \quad (78)$$

that is Eq. (35).

Acknowledgements We would like to thank G. Münster and A. Pelissetto for useful correspondence, and F. Gliozzi for fruitful discussions. This work was partially supported by the European Commission TMR programme ERBFMRX-CT96-0045.

References

- [1] See *e. g.* J. Zinn-Justin, *Quantum Field Theory and Critical Phenomena*, Oxford: Clarendon, 1990 and references therein.
- [2] M. Caselle and M. Hasenbusch, *J. Phys.* **A30** (1997) 4963.
- [3] J. Heitger, Diploma Thesis, University of Münster, 1993.
- [4] P. Provero, *Phys. Rev.* **E57** (1998) 3861.
- [5] A. S. Kronfeld *Nucl. Phys.* **B17** (Proceeding Supplement) (1990) 313.
M. Lüscher and U. Wolff, *Nucl. Phys.* **B339** (1990) 222.
- [6] M. Hasenbusch, K. Pinn and S. Vinti, hep-lat/9806012.
- [7] M. Hasenbusch, hep-lat/9902026.
- [8] V. Agostini, G. Carlino, M. Caselle and M. Hasenbusch, *Nucl. Phys.* **B484** (1997) 331.
- [9] H. Arisue and K. Tabata, *Nucl. Phys.* **B435** (1995) 555
- [10] M. Campostrini, A. Pelissetto, P. Rossi and E. Vicari *Phys. Rev.* **E57** (1998) 184

- [11] U. Wolff, Phys. Rev. Lett. **62** (1989) 361.
- [12] R. C. Brower and P. Tamayo, Phys. Rev. Lett. **62** (1989) 1087.
- [13] S. Klessinger and G. Münster, Nucl. Phys. **B386**(1992) 701.
- [14] M. Hasenbusch and K. Pinn, Physica **A245** (1997) 366.
- [15] A. K. Rajantie, Nucl. Phys. **B480** (1996) 729.
- [16] M. Lüscher and P. Weisz, Nucl. Phys. **B295** (1988) 65. K. Jansen *et al.*, Nucl. Phys. **B322** (1989) 698.
- [17] G. Münster and J. Heitger, Nucl. Phys. **B424** (1994) 582. C. Gutsfeld, J. Küster and G. Münster, Nucl. Phys. **B479** (1996) 654.